Brute Force Orientation and Alignment of Pyridazine Probed by Resonantly Enhanced Multiphoton Ionization

Hongzhi Li, Karen J. Franks, Rebecca J. Hanson, and Wei Kong*

Department of Chemistry, Oregon State University, Corvallis, Oregon 97331-4003

Received: February 27, 1998; In Final Form: July 1, 1998

Experimental measurements and theoretical calculations of brute force orientation in pyridazine (1,2-diazine) are discussed. The sample was prepared using supersonic expansion, and orientation was attempted via a strong uniform electric field. The electrostatic interaction between the permanent dipole moment and the electric field was sufficient to orient and align the molecular axes. Resonantly enhanced multiphoton ionization through the $\pi^* \leftarrow$ n transition was used to characterize the alignment of molecular axes. The permanent dipole moment of pyridazine is perpendicular to the transition dipole moment. As molecules became aligned in the orientation field, the transition dipole moments were perpendicular to the field. Enhancement of 40% in the excitation probability was observed when the polarization direction of the resonant laser was changed from parallel to perpendicular relative to the orientation field. Using a quantum mechanical approach, the experimental observation can be explained with satisfaction. Stark effects of the orientation field on energy levels, molecular axes, and electronic transitions were calculated using basis functions of symmetric tops. The calculation reproduced not only the overall variations in the absorption probability due to alignment but also the spectral shape of the electronic transition. This work demonstrates the feasibility of brute force orientation and has established the foundation for potential applications of this technique in studies of complex systems.

1. Introduction

Brute force orientation makes use of the electrostatic interaction between the permanent dipole moments of polar molecules and a uniform external electric field.[1−3] When this interaction is stronger than the rotational energy of the molecules, the potential barrier due to electrostatic interaction becomes unsurmountable. As a result, molecules are trapped within the barrier demonstrating hindered rotation or pendular motion, and their permanent dipole moments are oriented preferentially along the direction of the electric field. Orientation further induces alignment, and the permanent dipole moments of the polar molecules become parallel to the orientation field. The key to achieving brute force orientation is a low rotational temperature. Using supersonic expansion, successes of brute force orientation and alignment of polar molecules and clusters have been reported.[4−7]

Compared with other orientation and alignment approaches such as hexapole fields,[8−14] collision-induced processes,[15−18] and laser-related techniques,[19−26] superior qualities of brute force orientation include simplicity in experimental setup and universality in application. It only requires a uniform electric field and a supersonically cooled molecular beam, both of which can be achieved in a standard high-vacuum supersonic molecular beam apparatus. It can be applied to any type of polar molecule, including linear molecules, symmetric tops, and asymmetric tops. In some cases, even nonpolar molecules can be oriented using this method through clustering with polar species.[27]

Orientation and alignment of reactants provide an extra degree of control in reaction dynamics studies.[28,29] Through orientation achieved via hexapole fields and/or brute force fields, Loesch's and Stolte's groups have succeeded in investigating steric effects in bimolecular collisions.[30,31] In unimolecular reactions, dissociation of oriented parent molecules and clusters allows determination of the anisotropy of dissociative surfaces. Using brute force orientation, Miller's group investigated dissociation of van der Waals clusters.[32,33] They also reported that the strong electric field can not only orient the parent clusters in the space-fixed frame but also quench the tunneling motions of HF dimers.[34] When more than one potential surface is simultaneously accessible in a single-photon process, alignment of parent molecules allows polarization control of excitation. This ability can greatly simplify a complex dissociation process, lending itself to investigations of large systems.

Measurements of Stark levels of polar molecules in strong electric fields have been attempted.[4,35,36] However, detailed spectroscopic characterizations of this orientation and alignment effect have yet to be performed. In this paper, brute force orientation of pyridazine is investigated both experimentally and theoretically. From the variation of the transition probability under polarized excitation, distributions of molecular axes in an orientation field can be obtained. Resonantly enhanced multiphoton ionization (REMPI) of the nonfluorescing $\pi^* \leftarrow$ n transition of pyridazine is used to measure the transition probability. Two considerations make pyridazine an ideal system for this investigation: (1) it has a large permanent dipole moment of 4 D in its ground state, which makes it easy to achieve brute force orientation,[37] and (2) it has rotationally resolved ultraviolet absorption spectra, which allows determination of rotational temperatures of the supersonic molecular beam.[38,39]

* Corresponding author.

S1089-5639(98)01327-9 CCC: $15.00
Published on Web 09/26/1998

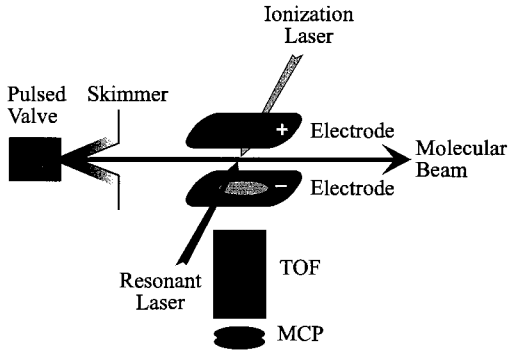

Figure 1. Experimental setup. The bottom electrode has a patch of mesh made of stainless steel for the extraction of cations from photoionization.

2. Experimental Section

The experimental apparatus was a standard molecular beam machine with a pulsed valve and a skimmer for supersonic cooling and collimating. Figure 1shows the arrangement of the molecular beam, the laser beams, and the orientation electrodes. Stainless steel plates of 12 × 20 × 6 mm were separated by 6 mm to generate a uniform electric field of up to 56 kV/cm. The center of the bottom electrode had a patch of mesh for ion transmission in the REMPI experiment. A time-of-flight mass spectrometer was placed underneath the electrodes, and the orientation field also served as the extraction field of the mass spectrometer. Pyridazine (Aldrich) was carried into the chamber by helium with a stagnation pressure of 1270 Torr. Under working conditions, the vacuum in the ionization chamber was 10^{-5} Torr. Based on the REMPI spectra obtained under field-free conditions, the rotational temperature of the molecular beam was 2 K.

In the $1 + 1'$ REMPI experiment, the first laser beam (termed the "resonant" beam in the following) at energies around 27 192 cm^{-1} was resonant with a vibronic transition ($16b^2_0$ band)[38,39] of pyridazine, while the second beam (termed the "ionization" beam) at 45 454 cm^{-1} supplied the energy for ionization. Pyridazine is known to undergo quick internal conversion, so the two dye lasers (LAS) were pumped by a single Nd:YAG laser (Spectra Physics) for synchronization in timing. Neither laser beam was focused, and no single laser signal from the resonant beam or the ionization beam was observable. Uniformity of the resonant laser beam proved to be crucial for avoiding partial saturation in the excitation step. A series of pinholes and collimation lenses were used to clean up the wave front. The polarization direction of the resonant laser was rotated by a Fresnel-Rhomb (CVI Lasers), while the polarization direction of the ionization laser was fixed perpendicular to the orientation field.

Figure 2 shows the REMPI spectra of pyridazine recorded when the orientation field was increased from 0 to 16 kV/cm. Both the resonant laser and the ionization laser were polarized perpendicular to the orientation field. As the field strength was increased to 8.5 kV/cm, transitions from lower rotational levels ($J'' \leq 2$) became broad. At 16 kV/cm, the whole spectrum was changed into a featureless transition. In the meantime, the overall vibronic band was shifted to a higher energy.

At an orientation field of 56 kV/cm, REMPI spectra recorded when the resonant laser was polarized parallel and perpendicular to the orientation field are shown in Figure 3. The two spectra show dramatic differences not only in their intensity distributions but also in overall transition strengths. To confirm that these differences are solely related to the orientation and alignment

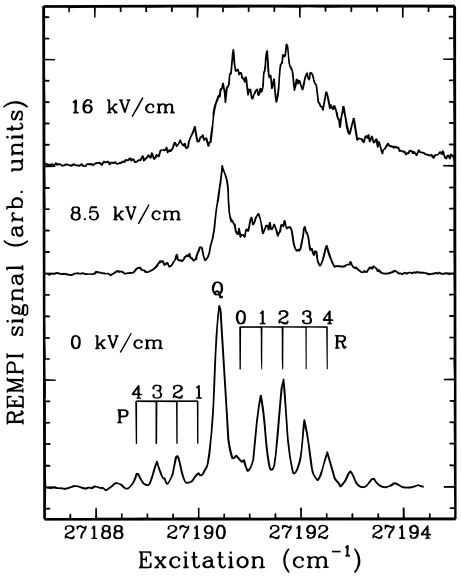

Figure 2. REMPI spectra of pyridazine showing the effect of orientation fields.

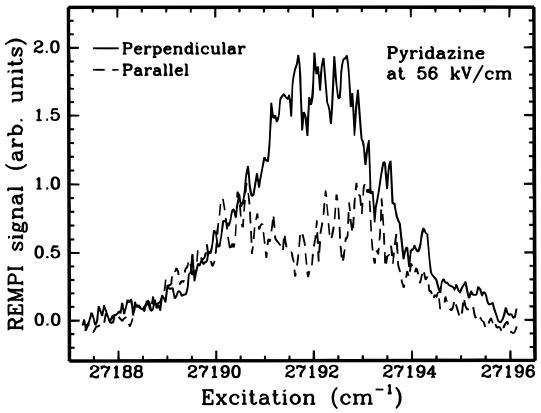

Figure 3. Polarization dependence of the REMPI spectra of pyridazine in an orientation field of 56 kV/cm. The two spectra were recorded when the polarization direction of the resonant laser was parallel or perpendicular to the orientation field.

effect of the electric field, the same comparison was made under field-free conditions. No differences between the spectra were observable without the orientation field, implying that the ionization step is independent of the alignment of pyridazine caused by the linearly polarized resonant laser. This is because the ionization step is a bound-to-continuum transition, and the transition dipole moment to the continuum has both parallel and perpendicular components. The ejected electrons in a photoionization step can carry excess angular momentum, resulting in near equal contributions from both the parallel and perpendicular transitions. Variations of the REMPI spectra under different polarization directions of the resonant laser were thus solely related to the efficiency of the first excitation step, which is directly affected by the alignment of the ground-state molecules.

When the resonant laser was polarized perpendicular to the orientation field, its electric field was perpendicular to the permanent dipole moment and parallel to the transition dipole moment. Excitation in this case should have a favorable efficiency, and the overall transition probability should be increased. Figure 4 shows the ratios of the overall transition intensities when the laser was polarized perpendicular and parallel to the orientation field. The continuous line represents calculation results using eq 12 of section 3.2. At 56 kV/cm,

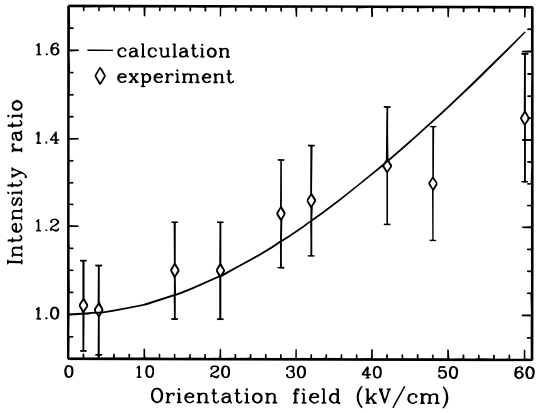

Figure 4. Effect of molecular alignment on the overall transition probabilities of pyridazine. The vertical axis shows ratios of the transition intensity when the polarization direction of the resonant laser was perpendicular and parallel to the orientation field. The transition dipole moment of pyridazine is perpendicular to its permanent dipole moment, which became aligned when the strength of the orientation field was increased.

the enhancement in the overall transition probability was 40% when the laser was changed from parallel to perpendicular to the orientation field. The ratio is unity under field-free conditions, confirming that the ionization laser was not probing the alignment effect induced by the resonant laser.

The uncertainty in the experimental data is partially caused by variations of the overlap between the two laser beams in this $1 + 1'$ REMPI experiment. The Fresnel-Rhomb that was used to rotate the polarization direction of the resonant laser would change both the position and direction of the output beam. In addition, the orientation field caused further fluctuations in the ion signal. We attribute this to instabilities in the experimental conditions, and we are in the process of further improvement. Saturation effects were observable from both the resonant laser and the ionization laser, and the results in Figure 4 were obtained with 0.2 mJ in the resonant laser and 8 μJ in the ionization laser (beam diameter 2 mm). At above 0.5 mJ in the resonant beam, power broadening effects became visible.

3. Theoretical Treatment

Detailed treatment of symmetric top and linear molecules in a uniform electric field has been given in the literature.[3, 40−43] Orientation of asymmetric top molecules was also investigated by Bulthuis et al.[44] They pointed out that energy levels of asymmetric top molecules exhibit avoided crossings as the orientation field is increased, while for symmetric top molecules these crossings are allowed for symmetry reasons. Depending on the time scale of molecular rotation and the rate of change of the Stark field exerted on the molecular beam, the probability of curve crossing will be different, and the final state distribution and therefore the molecular orientation will be different.

Although the theoretical background for electronic transitions of asymmetric top molecules in a strong Stark field has existed for a long time, a detailed calculation is still lacking due to its tedious nature. In this paper, we treat electronic transitions of asymmetric top molecules in a strong electric field using a full quantum mechanics approach. Neither the asymmetry nor the electric field is treated as a perturbation. Effects of alignment of molecular axes on intensity distributions and overall transition probabilities are investigated. The calculation uses pyridazine as a prototype, but the procedure can be adapted easily for any asymmetric top molecule.

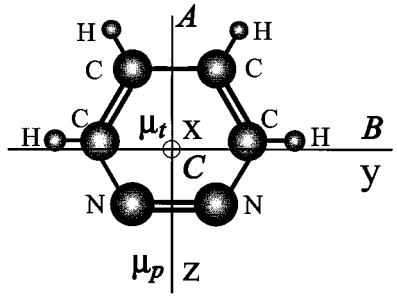

A	B	C	μp
0.208	0.199	0.102	4.14

Figure 5. Coordinate system of pyridazine. The rotational constants are in cm^{-1}, and the permanent dipole moment is in debye. The transition dipole moment is along the *C* axis perpendicular to the molecular plane, while the permanent dipole moment is along the *A* axis—the symmetry axis of the C_{2v} molecule.

3.1. Orientation and Alignment in a Brute Force Field. Figure 5 shows the coordinate system and the principal axis of pyridazine. Its rotational constants and permanent dipole moment are also listed in the same figure.[38] Under field-free conditions, pyridazine is a near-oblate symmetric top with the *C* axis as the principal axis. However, as an asymmetric top, the symmetry axis of this C_{2v} molecule is along the *A* axis, and the projection axis in the molecular frame should be *A* instead of *C*. Approximations using oblate symmetric top wave functions ($|JK_cM\rangle$) and transition intensities are acceptable under field-free conditions,[39,45,46] but a difficulty arises in association with nuclear statistics. The statistical weight is 13 for K_a = even and 11 for K_a = odd. For high *J* states, this ratio does not substantially affect the overall distribution of the transition intensities, but its effect on low *J* ($J \leq 3$) states is not negligible. In this calculation, the projection axis in the molecular frame is chosen to be along the direction of the permanent dipole moment. Consequently, prolate top wave functions ($|JK_aM\rangle$) are used as basis functions for this near-oblate-top molecule. The $^1B_1 \leftarrow {}^1A_1$ electronic transition of pyridazine has a transition dipole moment along the *C* axis, so the selection rule should be $\Delta K_a = \pm 1$ and $\Delta K_c = 0$ in this coordinate system. The quantization axis in the laboratory frame is along the orientation field.

Symmetry-adapted wave functions $|JKMs\rangle$ are used as basis functions:[47]

$$|JKMs\rangle = \frac{1}{\sqrt{2}}(|JKM\rangle + (-1)^s|J-KM\rangle), \quad (K > 0,\ s = 0 \text{ or } 1) \quad (1)$$

In an electric field, the magnetic quantum number *M* is the only good quantum number, and the total rotational angular momentum $\hat{J}$ is no longer conserved. The rotational wave function of the asymmetric top molecule is thus

$$|\tau M\rangle = \sum_{J,K,s} C^{\tau,M}_{J,K,s}|JKMs\rangle \quad (2)$$

where τ is a register for keeping track of the wave functions of the asymmetric top. States with $\pm M$ values are degenerate, so only positive *M* values are included. The expansion coefficients are obtained from diagnolization of the Hamiltonian matrix including terms related to the asymmetry and the electric field:

$$H = B\mathbf{J}^2 + (A - B)J_z^2 + \frac{C - B}{4}(J_+^2 + J_-^2 + J_+J_- + J_-J_+) + \boldsymbol{\mu}_p\cdot\mathbf{E} \quad (3)$$

The nonzero terms are (assuming that the permanent dipole moment $\boldsymbol{\mu}_p$ is along the A axis)

$$H_{JKs,JKs} = \frac{B + C}{2}[J(J + 1) - K^2] + AK^2$$

$$\left(\text{if } K = 1, \text{ an extra term of } (-1)^s\frac{C - B}{4}J(J + 1) \text{ needs to be added}\right) \quad (4)$$

$$H_{JK\pm2s,JKs} = \frac{C - B}{4}[J(J + 1) - (K \pm 1)(K \pm 2)]^{1/2} \times [J(J + 1) - K(K \pm 1)]^{1/2}$$

$$(\text{if } K = 0, \text{ the expression needs to be multiplied by } \sqrt{2}) \quad (5)$$

$$H_{JKs,J+1Ks} = -\frac{[(J + 1)^2 - K^2]^{1/2}[(J + 1)^2 - M^2]^{1/2}}{(J + 1)[(2J + 1)(2J + 3)]^{1/2}}\boldsymbol{\mu}_p\cdot\mathbf{E} \quad (6)$$

$$H_{JK0,JK1} = -\frac{MK}{J(J + 1)}\boldsymbol{\mu}_p\cdot\mathbf{E} \quad (7)$$

Equations 4−7 imply that, under field-free conditions, basis functions with the same J and s but different K quantum numbers will be mixed due to the asymmetry of the molecular system. The orientation field further results in mixing of basis functions with the same K and s but different J values or the same J and K but different s values. Under low fields, terms related to the occupied low-energy levels and a few higher levels are sufficient for an accurate calculation. However, as the field strength increases, more high-energy basis functions need to be taken into account, and to avoid truncation errors, the maximum J value included in the present calculation was $J_{max} = 20$. By recognizing the symmetry in the matrix elements, the calculation can be simplified. The Hamiltonian matrix is block diagonal for each M value. Within each submatrix of the same M value, terms with odd K values do not interact with those of even K values. The matrix can thus be further block diagonalized through reorganizing the basis functions into two group with K = odd or even.

Orientation and alignment obtained through the brute force field can be expressed in terms of angular momentum multipoles. In a cylindrically symmetric system (the orientation field as the symmetry axis), the distribution function ($P(\cos\theta)$) of the permanent dipole moment follows:

$$P(\cos\theta) = {}^1/_2(1 + \sum_{n=1}^{\infty} a_n P_n(\cos\theta)) \quad (8)$$

where a_1 represents orientation, a_2 represents alignment, and P_n are Legendre polynomials. For an asymmetric top molecule with wave functions expressed as eq 2, the values of a_n can be calculated using

$$a_n = \frac{(2n + 1)}{2}\sum_M N_M \sum_\tau e^{-E_{\tau M}/k_BT} \sum_{J_1,J_2,K,s_1,s_2} C^{\tau M}_{J_1Ks_1}C^{\tau M}_{J_2Ks_2} \times [1 + (-1)^{s_1+s_2+J_1+J_2+n}](-1)^{M-K}N_K\frac{[(2J_1 + 1)(2J_2 + 1)]^{1/2}}{2} \times \begin{pmatrix} J_2 & J_1 & n \\ M & -M & 0 \end{pmatrix}\begin{pmatrix} J_2 & J_1 & n \\ K & -K & 0 \end{pmatrix} \quad (9)$$

where $\begin{pmatrix} J_1 & J_2 & J_3 \\ M_1 & M_2 & M_3 \end{pmatrix}$ is a $3 - J$ symbol, N_M is the degeneracy for each M value, and N_K is the nuclear statistical weighting factor, i.e.

$$N_M = 2\ (M > 0), \quad N_M = 1\ (M = 0) \quad (10)$$

$$N_K = 13\ (K = \text{even}), \quad N_K = 11\ (K = \text{odd}) \quad (11)$$

The Boltzmann factor in eq 9 represents diabatic transformation as molecules move into the orientation field. This scenario is likely in experiments where the region of supersonic expansion is embedded in the orientation field. In most apparatus using free jet expansion without collimating skimmers, the electric field between the pulsed valve and the orientation electrodes is comparable to the orientation field. Supersonic cooling results in occupation of the lowest Stark manifolds, so the present treatment is appropriate. However, if a skimmer is used and the orientation field is shielded from the region of supersonic expansion, adiabatic transformation might be favorable. The present matrix diagonalization routine[48] makes it difficult for adiabatic treatment, and the effect of adiabaticity on molecular orientation is still under investigation.

Using values listed in Figure 5 for pyridazine, energies of the $J = 1$ levels are shown in Figure 6. The labeling has the format of $J_{Ka\ Kc}(M)$. Each $J_{Ka\ Kc}$ state is split into two sublevels with $M = 0$ and 1. Different $1_{Ka\ Kc}$ states have different symmetries; therefore, crossings between these curves are allowed even for this asymmetric top. Avoided crossings are uncommon in the case of pyridazine due to the similarity of its rotational constants to those of an oblate symmetric top. Some of the sublevels have elevated energies as the field is initially increased; however, all energy levels of the $J = 1$ manifold have decreased energies at high fields. For levels with higher J values, similar behavior can be observed, although to achieve the same Stark shift in energy, higher field strengths are required.

Figure 7 shows calculated distributions of the permanent dipole moment under three different orientation fields. Normalization was achieved by setting the area underneath the distribution function to unity. This treatment ignored any anistropy in the plane perpendicular to the orientation axis, since the orientation field should not have any direct impact in this plane. As the field strength increases, more molecules are oriented with their permanent dipole moments along the orientation field. Consequently, the molecular plane becomes parallel with the orientation field. At 60 kV/cm, twice as many molecules are aligned with the orientation field as are perpendicular to it. This corresponds to 70% of the pyridazine molecules having their nitrogen end preferentially pointing to the positive electrode, and about half of the molecules are restricted within a cone of 45° (half angle) surrounding the electric field.

Without the orientation field, the only nonzero multipole is a_0—the population term. As molecules become oriented by an electric field, the orientation multipole a_1 increases. With further increase of the field strength, the oriented ensemble starts to

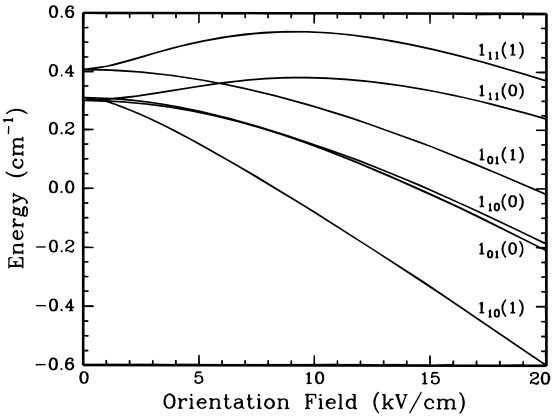

Figure 6. Effect of the orientation field on energy levels of the $J = 1$ states. The labeling follows $J_{Ka\ Kc}(M)$. Crossings shown in the figure are allowed for symmetry reasons.

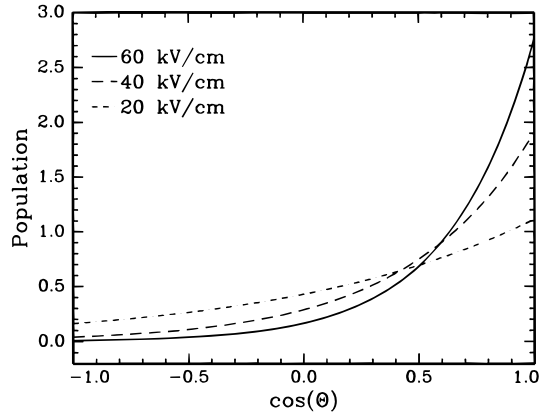

Figure 7. Distributions of the permanent dipole moment of pyridazine in orientation fields. The variable Θ refers to the angle between the orientation field and the permanent dipole moment. The values were normalized by setting the overall population (integrated area underneath the curve) to unity.

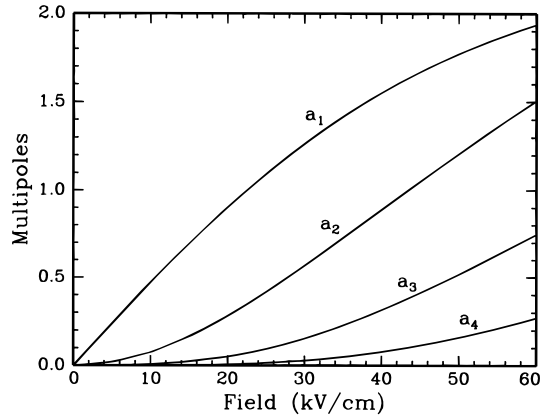

Figure 8. Variations of angular momentum multipoles with orientation fields. As molecules become oriented in an electric field, higher multipoles than a_0 (the population term) increase.

demonstrate alignment, and the a_2 multipole starts to increase. Figure 8 shows variations of the multipoles with the orientation field. At 60 kV/cm, multipoles as high as a_4 are nonnegligible.

3.2. Electronic Transition in a Strong Uniform Electric Field. To calculate transition probabilities between two electronic states, diagnolization of Hamiltonian matrices needs to be performed for both the ground and excited states. Assuming an electronic dipole moment transition, the intensity distribution is

$$I_{\tau_2 M_2 \leftarrow \tau_1 M_1} \propto \sum_p N_{M_1} e^{-E_{\tau_1 M_1}/k_B T} \Big| \sum_{J_2 K_2 S_2, J_1 K_1 S_1} {}^1/_2 C^{\tau_2 M_2}_{J_2 K_2 S_2} C^{\tau_1 M_1}_{J_1 K_1 S_1} \times (-1)^{M_1 - K_1} N_{K_1} \sum_q \mu_t(1,q)\, E(1,p) (-1)^{p-q} \begin{pmatrix} J_1 & J_2 & 1 \\ -M & M_2 & -p \end{pmatrix} \times \left[\begin{pmatrix} J_1 & J_2 & 1 \\ -K_1 & K_2 & q \end{pmatrix} + (-1)^{s_1} \begin{pmatrix} J_1 & J_2 & 1 \\ K_1 & K_2 & q \end{pmatrix} \right] \times [(-1)^{s_1+s_2+J_1+J_2} + 1][(2J_1+1)(2J_2+1)]^{1/2} \Big|^2 \quad (12)$$

where $\mu_t(1,q)$ and $E(1,p)$ are spherical tensor representations of the transition dipole moment and the laser field, respectively. When the transition dipole moment is along the C axis (x axis),

$$\mu_t(1,-1) = -\mu_t(1,1) = -\frac{1}{\sqrt{2}}; \quad \mu_t(1,0) = 0 \quad (13)$$

If the excitation laser is polarized perpendicular to the electric field,

$$E(1,-1) = E(1,1) = \frac{1}{\sqrt{2}}; \quad E(1,0) = 0 \quad (14)$$

Otherwise,

$$E(1,-1) = E(1,1) = 0; \quad E(1,0) = 1 \quad (15)$$

Without an orientation field, the total angular momentum quantum number J is a good quantum number, and eq 12 agrees with the general expression for an electronic dipole moment transition of asymmetric top molecules.[47] In an orientation field, the wave functions become polarized through mixing with other states of different J values. The effect of the orientation field is signified by the mixing coefficients in the wave function.

Figure 9 shows a REMPI spectrum of pyridazine recorded under field-free conditions from a free jet (no skimmer was used). Overlaid on the experimental data is the calculation result based on eq 12. The diatomic-like appearance of the spectrum is due to small changes in the C constant between the upper and lower states of this vibronic transition. At a rotational temperature of 1.0 K, the agreement between theory and experiment is remarkable. During the experiment, however, a skimmer was used, and insufficient pumping of the pulsed valve region resulted in an increased temperature of 2 K.

With the increase of the orientation field, Stark shifts in energy levels of both the ground and excited state result in splittings of each rovibronic transition. The selection rule is $\Delta M = 0$ (or ± 1) when the polarization direction of the resonant laser is parallel (or perpendicular) to the orientation field. The permanent dipole moment of the upper electronic state (2.8 D) is smaller than that of the ground state (4.1 D), so the decrease in energy due to the Stark effect for the upper state is smaller than that of the ground state. Consequently, the vibronic band was shifted to a higher energy, as seen in Figure 2 (section 2).

Figure 10 compares theory with experiment at a field strength of 56 kV/cm. The uncertainty in the excitation energy from the experimental spectra is ± 0.5 cm^{-1}, and both simulation spectra used the same energy shift as that under the field-free conditions in Figure 9. The same intensity factor was used for both polarization directions, and the agreement is satisfactory. When the laser was polarized along the orientation field (Figure 10a), the peak on the lower energy side was mainly composed of transitions of the original Q branch, while the higher energy side corresponded to the R branch. As the laser became perpendicular to the orientation field (Figure 10b), the higher energy side (R branch) showed a stronger enhancement effect,

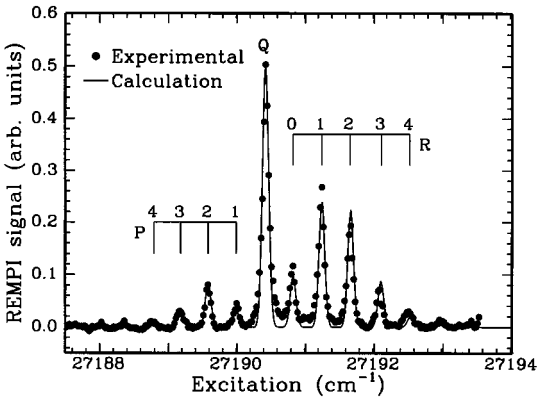

Figure 9. REMPI spectrum of pyridazine. The rotational temperature of the free jet expansion was 1 K, and the simulation was based on eq 12.

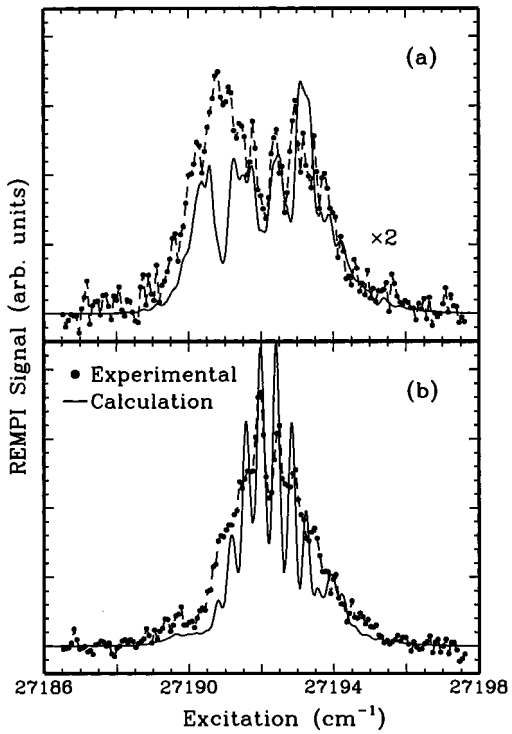

Figure 10. Comparison between theoretical and experimental spectra at an orientation field of 56 kV/cm. The polarization direction of the resonant laser was (a) parallel and (b) perpendicular to the orientation field. The calculation used the same intensity factor for both polarization directions.

and the overall transition intensity was also increased. The calculation correctly reproduced not only the overall shape, relative intensities, and the position of the transition but also some of the detailed structures of the spectra.

The ratios of the overall transition probabilities in Figure 4 were obtained by integrating the corresponding spectra. The agreement between experiment and theory is satisfactory. In this $1 + 1'$ REMPI process, the experimental measurement is only sensitive to the alignment mulitpole a_2 expanded in both the orientation direction (corresponding to Euler angle θ) and the transition dipole moment direction (perpendicular to the permanent dipole, corresponding to Euler angle χ). Effects of the orientation (a_1) and other higher multipoles (a_n, $n > 2$) are not detectable in a resonant single-photon process using linearly polarized lasers. It is worth noting that although the rotational temperature of the molecular beam was 2 K, a few rotational levels ($J \leq 5$) were occupied. These levels were neither oriented uniformly in the electric field, nor did they have the same transition probability. Levels with lower J values had better orientation, but lower transition intensity. The resulting enhancement in the overall transition probability is therefore smaller than that calculated from projections of molecular axes following the distribution of Figure 7.

4. Concluding Remarks

This work demonstrated the feasibility and characterized the extent of molecular alignment through a uniform electric field. From dependence of the overall transition probability on the polarization direction of a linearly polarized laser, distributions of molecular axes were obtained. At a field strength of 56 kV/cm, the ionization efficiency from $1 + 1'$ REMPI of pyridazine was enhanced by 40% as the polarization direction of the resonant laser was changed from parallel to perpendicular to the orientation field. Theoretical modeling of the Stark levels, transition intensity distributions, and overall transition probabilities resulted in good agreement with experimental observations.

An advantage of brute force orientation is its high particle density resulting from orientation of all the molecules in a supersonic beam. In contrast, orientation by hexapole fields or laser processes is typically achieved through state selection. Furthermore, the simplicity and low cost in experimental setup using brute force orientation are particularly attractive. The present experiment demonstrates that, for any polar molecule or cluster with a permanent dipole moment of a few debye, brute force orientation is within reach in most laboratories using supersonic molecular beams in high-vacuum systems.

Acknowledgment. This work was supported by the National Science Foundation, Division of Chemistry through the Faculty Early Career Development Program. The authors are in debt to the help from Dr. R. E. Miller and D. Moore for discussions on the calculation, in particular, for their generous supply of high-resolution experimental spectra to debug the computer program.

References and Notes

(1) Friedrich, B.; Herschbach, D. R. *Nature* **1991**, *353*, 412.
(2) Stolte, S. *Nature* **1991**, *353*, 391.
(3) Loesch, H. J.; Remscheid, A. *J. Chem. Phys.* **1990**, *93*, 4779.
(4) Block, P. A.; Bohac, E. J.; Miller, R. E. *Phys. Rev. Lett.* **1992**, *68*, 1303.
(5) Van Leuken, J. J.; Bulthuis, J.; Stolte, S.; Loesch, H. J. *J. Phys. Chem.* **1996**, *100*, 16066.
(6) Loesch, H. J.; Remscheid, A. *J. Phys. Chem.* **1991**, *95*, 8194.
(7) Friedrich, B.; Herschbach, D. R.; Rost, J.-M.; Rubahn, H.-G.; Renger, M.; Verbeek, M. *J. Chem. Soc., Faraday Trans.* **1993**, *89*, 1539.
(8) Parker, D. H.; Bernstein, R. B. *Annu. Rev. Phys. Chem.* **1989**, *40*, 561.
(9) Jones, E. M.; Brooks, P. R. *J. Chem. Phys.* **1970**, *53*, 55.
(10) Böwering, N.; Volkmer, M.; Meier, C.; Lieschke, J.; Fink, M. *Z. Phys. D* **1994**, *30*, 177.
(11) Janssen, M. H. M.; Parker, D. H.; Stolte, S. *J. Phys. Chem.* **1991**, *95*, 8142.
(12) Hain, T. D.; Weibel, M. A.; Backstrand, K. M.; Pope, P. E.; Curtiss, T. J. *Chem. Phys. Lett.* **1996**, *262*, 723.
(13) Ohoyama, H.; Ogawa, T.; Makita, H.; Kasai, T.; Kuwata, K. *J. Phys. Chem.* **1996**, *100*, 4729.
(14) Bulthuis, J.; van Leuken, J.; Stolte, S. *J. Chem. Soc., Faraday Trans.* **1995**, *91*, 205.
(15) Saleh, H. J.; McCaffery, A. J. *J. Chem. Soc., Faraday Trans*. **1993**, *89*, 3217.
(16) Weida, M. J.; Nesbitt, D. J. *J. Chem. Phys.* **1994**, *100*, 6372.
(17) Aqullanti, V.; Ascenzi, D.; Cappelletti, D.; Pirani, F. *Nature* **1994**, *371*, 398.
(18) Neitzke, H.-P.; Terlutter, R. *J. Phys. B: At. Mol. Opt. Phys.* **1992**, *25*, 1931.
(19) Weida, M. J.; Parmenter, C. S. *J. Chem. Phys.* **1997**, *107*, 7138.

(20) Zare, R. N. *Ber. Bunsen-Ges. Phys. Chem.* **1982**, *86*, 422.
(21) Smith, C. J.; Spain, E. M.; Dalberth, M. J.; Leone, S. R.; Driessen, J. P. J. *J. Chem. Soc., Faraday Trans.* **1989**, *85*, 925.
(22) Friedrich, B.; Herschbach, D. *J. Phys. Chem.* **1995**, *99*, 15686.
(23) DeVries, M. S.; Tyndall, G. W.; Cobb, C. L.; Martin, R. M. *J. Chem. Phys.* **1987**, *86*, 2653.
(24) Bhardwaj, V. R.; Vijayalakshmi, K.; Mathur, D. *Phys. Rev. A* **1997**, *56*, 2455.
(25) Kim, W.; Felker, P. M. *J. Chem. Phys.* **1996**, *104*, 1147.
(26) Vrakking, M. J. J.; Stolte, S. *Chem. Phys. Lett.* **1997**, *271*, 209.
(27) Bemish, R. J.; Bohac, E. J.; Wu, M.; Miller, R. E. *J. Chem. Phys.* **1994**, *101*, 9457.
(28) Stolte, S. *Ber. Bunsen-Ges. Phys. Chem.* **1982**, *86*, 413.
(29) Loesch, H. J. *Annu. Rev. Phys. Chem.* **1995**, *46*, 555.
(30) Loesch, H. J.; Möller, J. *J. Phys. Chem.* **1997**, *101*, 7534.
(31) Janssen, M. H. M.; Mastenbroek, J. W. G.; Stolte, S. *J. Phys. Chem. A* **1997**, *101*, 7605.
(32) Oudejans, L.; Miller, R. E. *J. Phys. Chem.* **1995**, *99*, 13670.
(33) Oudejans, L.; Miller, R. E. *J. Phys. Chem. A* **1997**, *101*, 7582.
(34) Bemish, R. J.; Chan, M. C.; Miller, R. E. *Chem. Phys. Lett.* **1996**, *251*, 182.
(35) Durand, A.; Loison, J. C.; Vigué, J. *J. Chem. Phys.* **1994**, *101*, 3514.
(36) Slenczka, A.; Friedrich, B.; Herschbach, D. *Chem. Phys. Lett.* **1994**, *224*, 238.
(37) Schneider, W. C. *J. Am. Chem. Soc.* **1948**, *70*, 627.
(38) Innes, K. K.; Ross, I. G.; Moomaw, W. R. *J. Mol. Spectrosc.* **1988**, *132*, 492.
(39) Li, H.; Kong, W. *J. Chem. Phys.* **1998**, *109*, 4782.
(40) Bulthuis, J.; van Leuken, J.; van Amerom, F.; Stolte, S. *Chem. Phys. Lett.* **1994**, *222*, 378.
(41) Rost, J. M.; Griffin, J. C.; Friedrich, B.; Herschbach, D. R. *Phys. Rev. Lett.* **1992**, *68*, 1299.
(42) Maergoiz, A. I.; Troe, J.; Weiss, Ch. *J. Chem. Phys.* **1994**, *101*, 1885.
(43) Loison, J. C.; Durand, A.; Bazalgette, G.; White, R.; Audouard, E.; Vigué, J. *J. Phys. Chem.* **1995**, *99*, 13591.
(44) Bulthuis, J.; Möller, J.; Loesch, H. J. *J. Phys. Chem. A* **1997**, *101*, 7684.
(45) Li, H.; Kong, W. *J. Chem. Phys.* **1997**, *107*, 3774.
(46) Li, H.; Depre, P.; Kong, W. *Chem. Phys. Lett.* **1997**, *273*, 272.
(47) Zare, R. N. *Angular Momentum*; Wiley-Interscience: New York, 1988.
(48) Wilkinson, J. H.; Reinsch, C. *Handbook for Automatic Computation*; Springer-Verlag: New York, 1971; Vol. 2.